

Formation and Mechanical Properties of $\text{Mg}_{97}\text{Zn}_1\text{RE}_2$ Alloys with Long-Period Stacking Ordered Structure

Yoshihito Kawamura and Michiaki Yamasaki

Department of Materials Science and Engineering, Kumamoto University, Kumamoto 860-8555, Japan

We investigated the formation and mechanical properties of $\text{Mg}_{97}\text{Zn}_1\text{RE}_2$ alloys with long-period stacking ordered (LPSO) structures by examining RE = Y, La, Ce, Pr, Sm, Nd, Gd, Dy, Ho, Er, Tb, Tm and Yb. The LPSO phase developed for RE = Y, Dy, Ho, Er, Gd, Tb and Tm. LPSO Mg-Zn-RE alloys are either type I, in which the LPSO phase forms during solidification: Mg-Zn-Y, Mg-Zn-Dy, Mg-Zn-Ho, Mg-Zn-Er and Mg-Zn-Tm, or type II, in which the LPSO phase is nonexistent in as-cast ingots but precipitates with soaking at 773 K: Mg-Zn-Gd and Mg-Zn-Tb. The criteria for REs that form an LPSO phase in Mg-Zn-RE alloys are discussed. Mg-Zn-RE alloys with an LPSO phase, which were worked by hot extrusion, include high strength both at ambient and elevated temperatures, and good ductility. Their tensile yield strength, ultimate strength and elongation were 342–377 MPa, 372–410 MPa and 3–9%, respectively at ambient temperature, and 292–310 MPa, 322–345 MPa and 4–13% at 473 K. The LPSO Mg-Zn-RE alloys are promising candidates for lightweight structural materials.
[doi:10.2320/matertrans.MER2007142]

(Received June 22, 2007; Accepted August 22, 2007; Published October 18, 2007)

Keywords: magnesium-zinc-rare earth, long-period stacking ordered structure, structural material, mechanical properties

1. Introduction

In 2001, the alloy $\text{Mg}_{97}\text{Zn}_1\text{Y}_2$ (at%) was produced by rapidly solidified powder metallurgy, and displayed a yield strength of 610 MPa and elongation of 5% at room temperature, and a yield strength of 300 MPa at 473 K.¹⁾ The $\text{Mg}_{97}\text{Zn}_1\text{Y}_2$ alloy was composed mainly of α -Mg and Mg_{12}ZnY with a novel long-period stacking ordered (LPSO) structure. The LPSO structure was 18R, in which both Y and Zn were enriched in two atomic layers at 6 period intervals.^{2,3)} Moreover, the LPSO structure has been reported to have high thermal stability, and to be formed in cast ingots as well as in rapidly solidified alloys.^{4–6)} The LPSO structure was 18R in the as-cast state and a soaking at 773 K induced a change to a 14H structure, in which both Y and Zn were enriched in two atomic layers at 7 period intervals. The LPSO Mg-Zn-Y cast alloys that were hot-extruded exhibited high yield strength (>350 MPa) and reasonable elongation (>5%) at room temperature, and high yield strength (>300 MPa) at 473 K.^{6,7)} Recently, it has been reported that an LPO phase was formed in Mg-Zn-Gd alloys and the hot-extruded LPSO Mg-Zn-Gd alloys exhibited high strength at both ambient and elevated temperatures. Though the Mg-Zn-Gd alloys contained no LPSO phase and were composed of α -Mg and the intermetallic compound Mg_3Gd in the as-cast state, an LPSO phase with a 14H structure precipitated with soaking at 773 K for 10 h.^{8,9)} The formation process of an LPSO phase in the Mg-Zn-Gd alloys differs from that in the Mg-Zn-Y alloys. The LPSO magnesium alloys, therefore, can be classified into two types. Mg-Zn-Y alloys belong to type I, where the LPSO phase is formed during solidification, while Mg-Zn-Gd alloys are type II, in which the LPSO phase precipitates with soaking. There are 17 rare-earth (RE) metals, and new LPSO magnesium alloys with high mechanical performance are expected to be found among the Mg-Zn-RE alloys.

In this study, the formation and mechanical properties of LPSO $\text{Mg}_{97}\text{Zn}_1\text{RE}_2$ alloys were systematically investigated for RE = Y, La, Ce, Pr, Nd, Sm, Eu, Gd, Tb, Dy, Ho, Er, Tm and Yb.

2. Experimental Procedure

$\text{Mg}_{97}\text{Zn}_1\text{RE}_2$ (at%) cast ingots were produced by induction melting of pure Mg, Zn and RE metals in a carbon crucible. The RE metals were Y, La, Ce, Pr, Nd, Sm, Eu, Gd, Tb, Dy, Ho, Er, Tm and Yb. The molten alloys were cast in a steel die with a hole of 30 mm in diameter and 100 mm length in an argon atmosphere. Some cast ingots were soaked at 773 K for 10 hr in air. These ingots were machined into round bars of 29 mm in diameter and 70 mm length. The round billets were extruded at an extrusion ratio of 10, an extrusion temperature of 623 K, and a ram speed of 2.5 mm/s. The structure of the alloys was investigated by X-ray diffraction (XRD), scanning electron microscopy (SEM) and transmission electron microscopy (TEM). Tensile tests were carried out using an Instron-type tensile testing machine at room and elevated temperatures with an initial strain rate of $5 \times 10^{-4} \text{ s}^{-1}$. The diameter and gauge length of tensile samples were 3.0 mm and 25 mm, respectively for ambient-temperature tests, and 2.0 mm and 10 mm, respectively for elevated-temperature tests. In ambient-temperature testing, strain was measured using an electrical strain gauge. The tensile axis was along the direction of extrusion. The 0.2% proof strength was employed as yield strength.

3. Results

3.1 Microstructure of as-cast and soaked alloys

3.1.1 As-cast alloys

Figure 1 shows SEM micrographs of the as-cast $\text{Mg}_{97}\text{Zn}_1\text{RE}_2$ alloys. A secondary phase with a lamellar contrast was observed in the grain boundaries and dendrite arm boundaries for RE = Y, Dy, Ho, Er and Tm. The secondary phase of $\text{Mg}_{97}\text{Zn}_1\text{RE}_2$ alloys with RE = La, Ce, Pr, Nd, Sm, Eu and Yb had a sharp and smooth interface. The $\text{Mg}_{97}\text{Zn}_1\text{RE}_2$ cast alloys with RE = Y, Gd, Tb, Dy, Ho, Er and Tm exhibited pale contrast in the vicinity of bright contrast at the cell boundaries. X-ray diffraction patterns showed that the alloys were composed mainly of α -Mg and

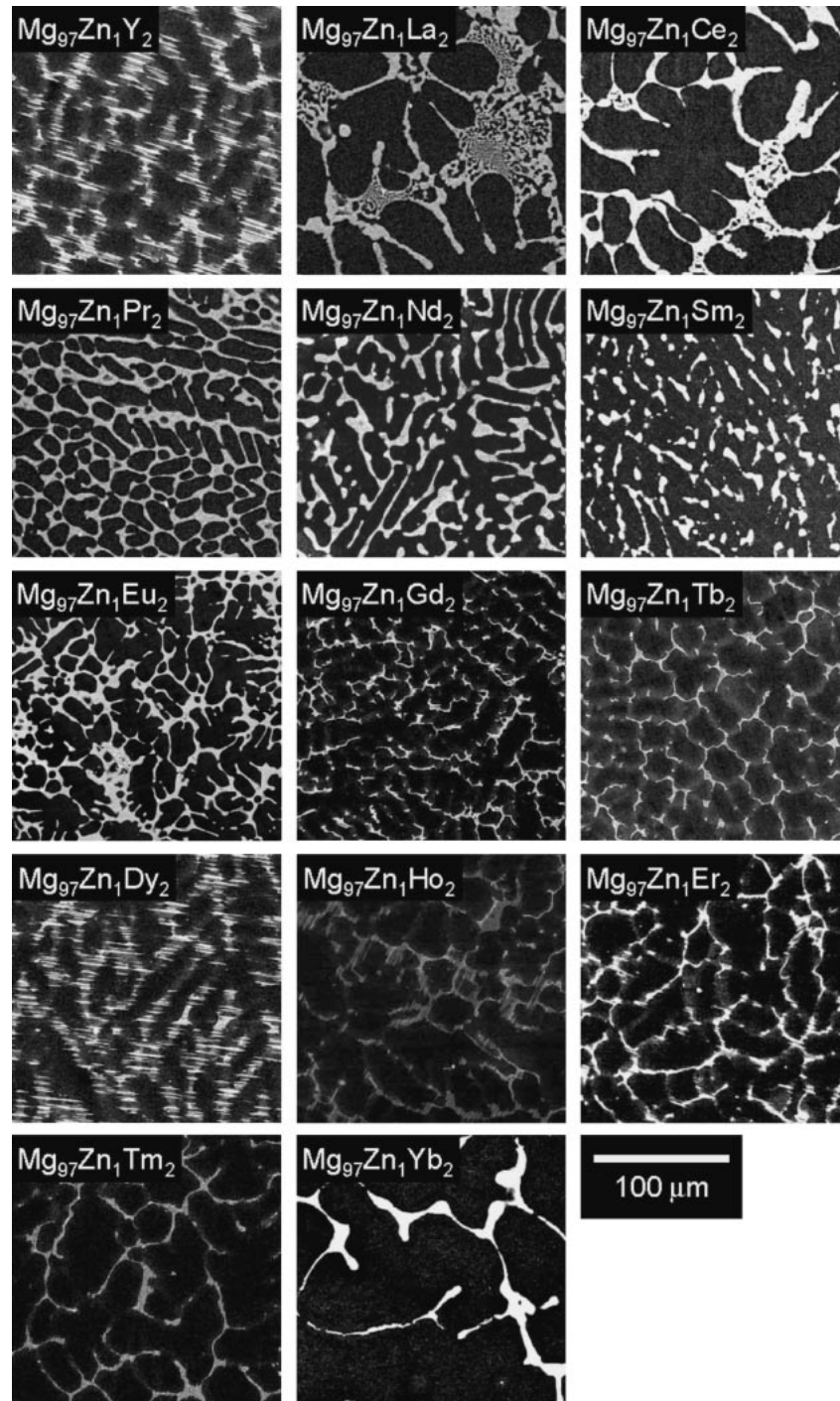


Fig. 1 SEM micrographs of as-cast $\text{Mg}_{97}\text{Zn}_1\text{RE}_2$ alloys.

Mg-RE intermetallic compounds for RE = La, Ce, Pr, Nd, Sm, Eu, Gd, Tb and Yb. In contrast, the Mg-Zn-Y, Mg-Zn-Dy, Mg-Zn-Ho, Mg-Zn-Er and Mg-Zn-Tm alloys exhibited X-ray diffraction peaks corresponding to an LPSO phase. Figure 2 shows the TEM micrographs and selected area electron diffraction (SAED) patterns of the as-cast $\text{Mg}_{97}\text{Zn}_1\text{Y}_2$, $\text{Mg}_{97}\text{Zn}_1\text{Dy}_2$, $\text{Mg}_{97}\text{Zn}_1\text{Ho}_2$, $\text{Mg}_{97}\text{Zn}_1\text{Er}_2$ and $\text{Mg}_{97}\text{Zn}_1\text{Tm}_2$ alloys, where a lamellar phase was formed around the cell boundaries. These TEM micrographs show the formation of an LPSO phase in these alloys. The LPSO structure was evaluated to be the 18R type in $\text{Mg}_{97}\text{Zn}_1\text{Y}_2$, $\text{Mg}_{97}\text{Zn}_1\text{Dy}_2$, $\text{Mg}_{97}\text{Zn}_1\text{Er}_2$ and $\text{Mg}_{97}\text{Zn}_1\text{Tm}_2$ alloys. An

LPSO structure of the 14H type coexisted with the 18R type in the $\text{Mg}_{97}\text{Zn}_1\text{Ho}_2$ alloy.

3.1.2 Soaked alloys

Figure 3 shows SEM micrographs of the $\text{Mg}_{97}\text{Zn}_1\text{RE}_2$ alloys soaked at 773 K for 10 h. A lamellar structure was still observed in the soaked $\text{Mg}_{97}\text{Zn}_1\text{RE}_2$ alloys with RE = Y, Dy, Ho, Er and Tm. A secondary phase with a sharp and smooth interface was maintained after soaking for RE = La, Ce, Pr, Nd, Sm, Eu and Yb. A lamellar structure appeared in the grain boundaries and dendrite arm boundaries by soaking in the $\text{Mg}_{97}\text{Zn}_1\text{RE}_2$ alloys with RE = Gd and Tb. It was revealed by X-ray diffraction patterns that the soaked

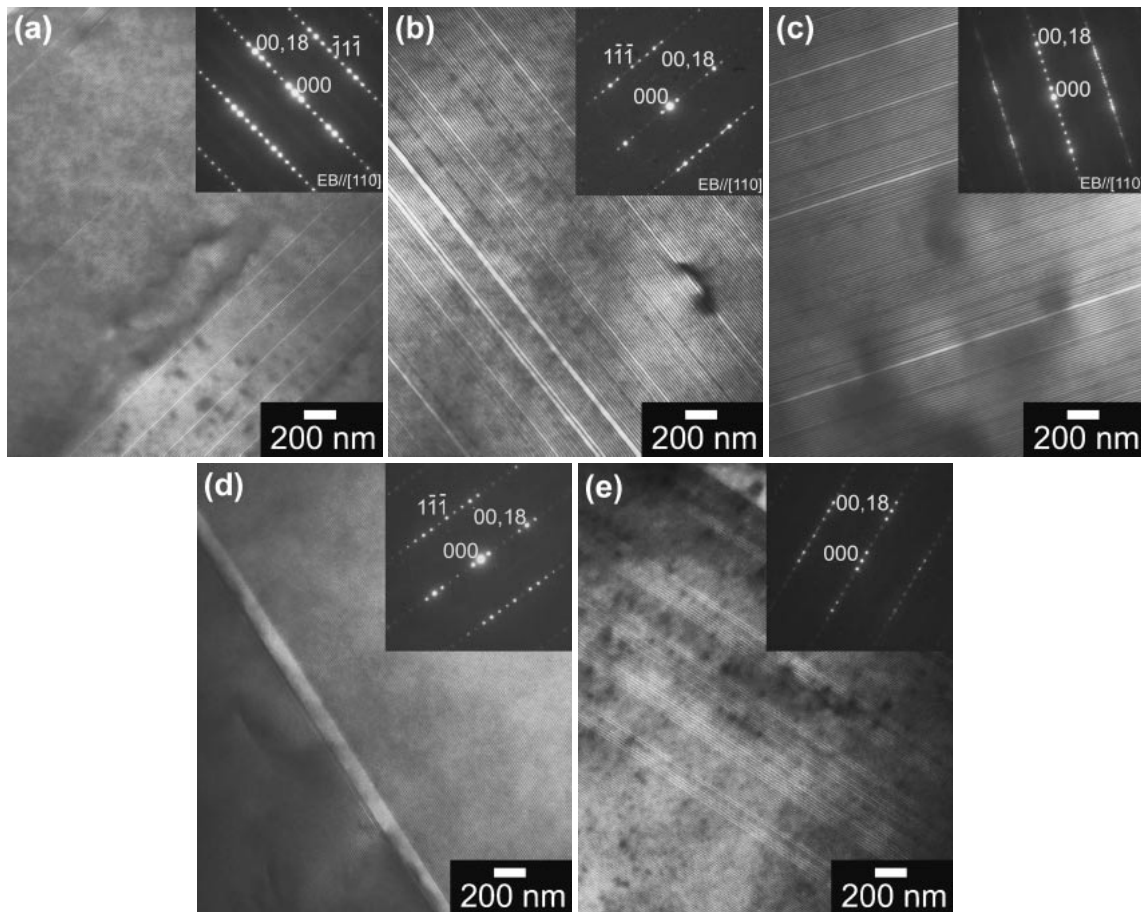


Fig. 2 TEM micrographs and SAED patterns of the LPSO phase formed in as-cast $\text{Mg}_{97}\text{Zn}_1\text{RE}_2$ alloys with RE = (a) Y, (b) Dy, (c) Ho, (d) Er and (e) Tm.

$\text{Mg}_{97}\text{Zn}_1\text{RE}_2$ alloys with RE = La, Ce, Pr, Nd, Sm, Eu and Yb were composed mainly of α -Mg and Mg-RE intermetallic compounds. In contrast, the soaked Mg-Zn-Gd and Mg-Zn-Tb alloys, which showed a lamellar contrast in the SEM micrograph, exhibited X-ray diffraction peaks corresponding to an LPSO phase, as well as the soaked Mg-Zn-Y, Mg-Zn-Dy, Mg-Zn-Ho, Mg-Zn-Er and Mg-Zn-Tm alloys. Figure 4 shows the TEM micrographs and SAED patterns of the soaked $\text{Mg}_{97}\text{Zn}_1\text{Gd}_2$ and $\text{Mg}_{97}\text{Zn}_1\text{Tb}_2$ alloys. The LPSO structure was evaluated to be the 14H type in the soaked $\text{Mg}_{97}\text{Zn}_1\text{Gd}_2$ and $\text{Mg}_{97}\text{Zn}_1\text{Tb}_2$ alloys. It was revealed that an LPSO phase was precipitated by soaking in the Mg-Zn-Gd and Mg-Zn-Tb alloys. Figure 5 shows the TEM micrographs and SAED patterns of the soaked $\text{Mg}_{97}\text{Zn}_1\text{Y}_2$, $\text{Mg}_{97}\text{Zn}_1\text{Dy}_2$, $\text{Mg}_{97}\text{Zn}_1\text{Ho}_2$, $\text{Mg}_{97}\text{Zn}_1\text{Er}_2$ and $\text{Mg}_{97}\text{Zn}_1\text{Tm}_2$ alloys that have an LPSO phase in the as-cast state. These TEM micrographs show that the LPSO phase of these soaked alloys was a 14H structure in the $\text{Mg}_{97}\text{Zn}_1\text{Y}_2$, $\text{Mg}_{97}\text{Zn}_1\text{Dy}_2$, $\text{Mg}_{97}\text{Zn}_1\text{Ho}_2$ and $\text{Mg}_{97}\text{Zn}_1\text{Er}_2$ alloys and an 18R type in the $\text{Mg}_{97}\text{Zn}_1\text{Tm}_2$ alloy.

3.2 Mechanical properties of wrought $\text{Mg}_{97}\text{Zn}_1\text{RE}_2$ alloys

Figure 6 shows the ambient-temperature tensile properties of wrought $\text{Mg}_{97}\text{Zn}_1\text{RE}_2$ alloys, which were prepared by hot extrusion of the soaked alloys. It should be pointed out that the wrought alloys with an LPSO phase have both high

strength and good ductility. The yield strength, ultimate tensile strength and elongation of the wrought alloys with an LPSO phase were more than 342 MPa, 372 MPa and 3%, respectively. In contrast, it was impossible to obtain concurrently both high strength and good ductility in any of the wrought alloys without an LPSO phase. Figure 7 shows the elevated-temperature tensile properties of the wrought $\text{Mg}_{97}\text{Zn}_1\text{RE}_2$ alloys, which were prepared by hot extrusion of the soaked alloys. The testing temperature was 473 K. The wrought $\text{Mg}_{97}\text{Zn}_1\text{RE}_2$ alloys with an LPSO phase exhibited a yield strength above 292 MPa, ultimate tensile strength above 322 MPa and elongation of 4% or more. It should be noted that the wrought alloys with an LPSO phase exhibited higher elevated-temperature strength than non-LPSO alloys. It is clear that the mechanical properties of the wrought LPSO Mg-Zn-RE alloys displayed high strength and good ductility at ambient and elevated temperatures.

4. Discussion

4.1 Classification of Mg-Zn-RE alloys

The LPSO $\text{Mg}_{97}\text{Zn}_1\text{RE}_2$ alloys can be classified into two types as shown in Table 1. In $\text{Mg}_{97}\text{Zn}_1\text{RE}_2$ alloys with RE = Y, Dy, Ho, Er and Tm, an LPSO phase was formed during solidification, and its structure transformed to a 14H type by soaking at 773 K except for Tm. In $\text{Mg}_{97}\text{Zn}_1\text{RE}_2$ alloys where RE = Gd and Tb, though Mg-RE intermetallic

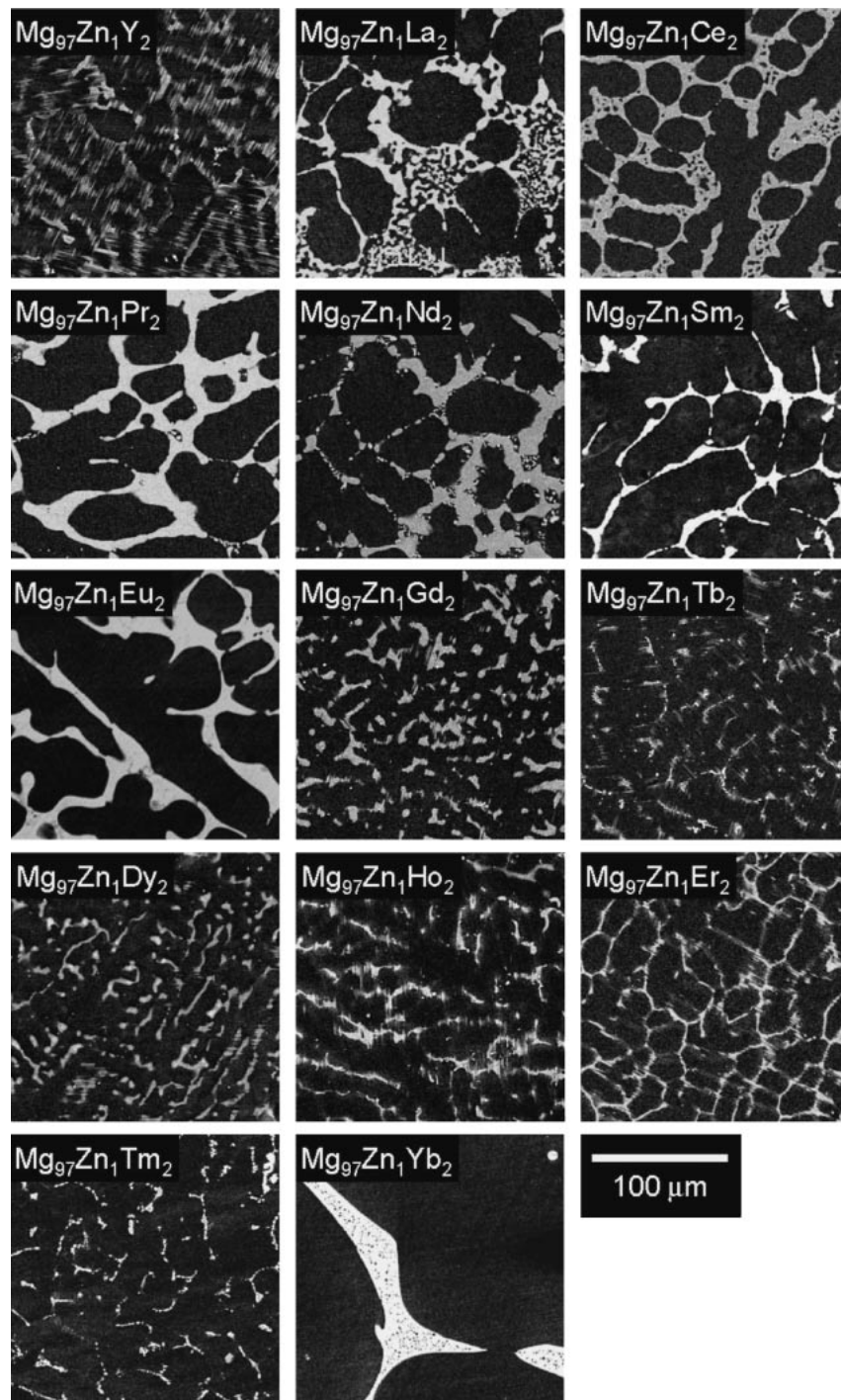


Fig. 3 SEM micrographs of the soaked $\text{Mg}_{97}\text{Zn}_1\text{RE}_2$ alloys.

compounds were formed during solidification and no LPSO phase existed in the as-cast state, a 14H LPSO phase was precipitated by soaking at 773 K. The former LPSO Mg-Zn-RE alloys can be classified as type I and the latter ones as type II. It is well known that Mg-Zn-RE alloys have been commercialized as heat-resistant alloys of the ZE or EZ series.¹⁰⁾ The RE elements used in the EZ and ZE alloys are, however, mischmetal composed of multiple RE elements containing mainly Ce, La and Nd. Therefore, these alloys can be classified as non-LPSO Mg-Zn-RE alloys. It can be said that the Mg-Zn-RE alloys with an LPSO phase are new heat-resistant magnesium alloys.

4.2 Criteria for RE elements forming an LPSO phase in Mg-Zn-RE alloys

Every pair among Mg, Zn and RE has negative mixing enthalpy, with an especially large negative mixing enthalpy for the Zn-RE pair. However, there is no distinct difference between RE elements.¹¹⁾ An LPSO phase only forms in Mg-Zn-RE alloys with REs having a hexagonal closed packed (HCP) structure that is the same as Mg and Zn. The RE elements of non-LPSO Mg-Zn-RE alloys are hexagonal (HEX), face centered cubic (FCC), body centered cubic (BCC) or rhombic.¹²⁾ The solid solubility limit of RE elements in magnesium is shown in Fig. 8.¹³⁾ The RE

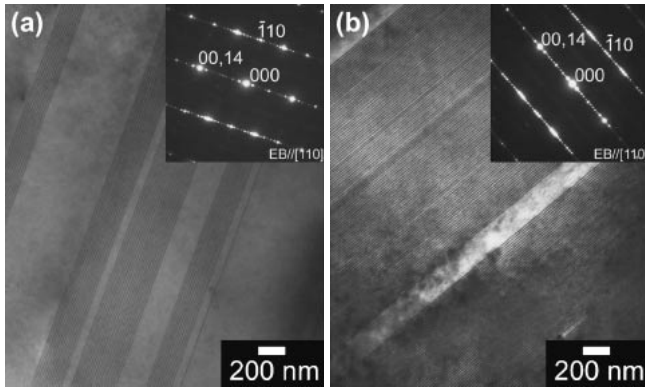


Fig. 4 TEM micrographs and SAED patterns of the LPSO phase in soaked (a) $\text{Mg}_{97}\text{Zn}_1\text{Gd}_2$ and (b) $\text{Mg}_{97}\text{Zn}_1\text{Tb}_2$ alloys.

elements in LPSO Mg-Zn-RE alloys have solid solubilities ranging from 3.75 to 6.9 at% in magnesium. In contrast, the RE elements in non-LPSO Mg-Zn-RE alloys have smaller solid solubilities, below 1.2 at% in magnesium. In particular, the solid solubility of La, Ce, Pr, Nd, Sm and Eu is 0.2 at% or less. The difference in atomic size between Mg, Zn and RE is large. Atoms of the RE elements of LPSO Mg-Zn-RE alloys are larger than Mg atoms by 8.4 to 11.9%, as shown in Fig. 9.¹²⁾ The atoms of the RE elements of non-LPSO Mg-Zn-RE alloys are, however, larger than Mg by more than 12.2%.

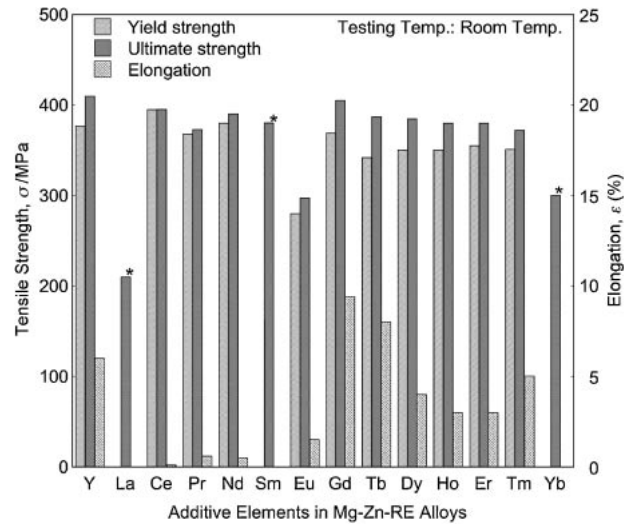


Fig. 6 Ambient-temperature tensile properties of extruded $\text{Mg}_{97}\text{Zn}_1\text{RE}_2$ alloys. The alloys shown in figure by asterisk mark, that is, Mg-Zn-La, Mg-Zn-Sm, and Mg-Zn-Yb, were broken in the elasticity limit. Fracture of the Mg-Zn-La, Mg-Zn-Ce and Mg-Zn-Yb alloys occurred in elastic deformation region.

Accordingly, the criteria for RE that will participate in forming an LPSO phase in Mg-Zn-RE alloys can be expressed as follows: (1) negative mixing enthalpy for Mg-RE and Zn-RE pairs, (2) HCP structure at room temperature,

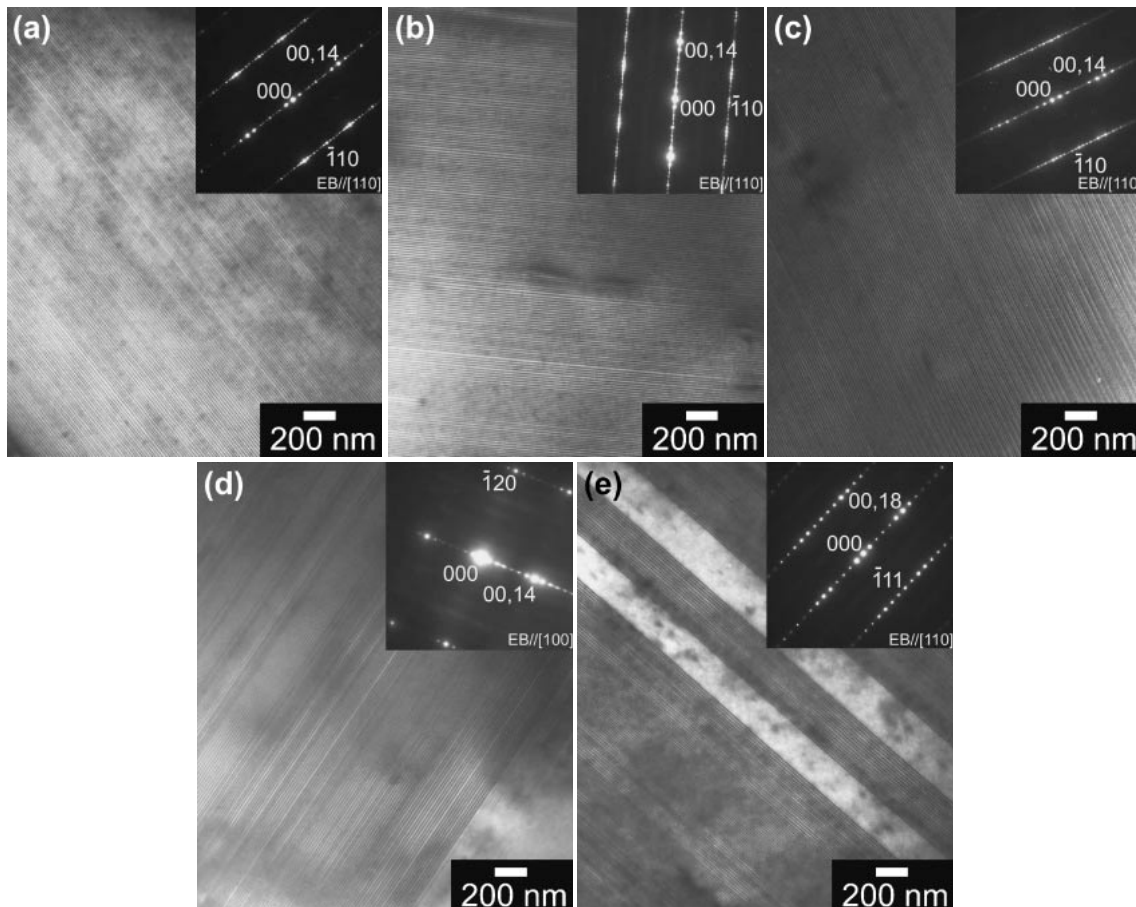


Fig. 5 TEM micrographs and SAED patterns of the LPSO phase in soaked (a) $\text{Mg}_{97}\text{Zn}_1\text{Y}_2$, (b) $\text{Mg}_{97}\text{Zn}_1\text{Dy}_2$, (c) $\text{Mg}_{97}\text{Zn}_1\text{Ho}_2$, (d) $\text{Mg}_{97}\text{Zn}_1\text{Er}_2$ and (e) $\text{Mg}_{97}\text{Zn}_1\text{Tm}_2$ alloys.

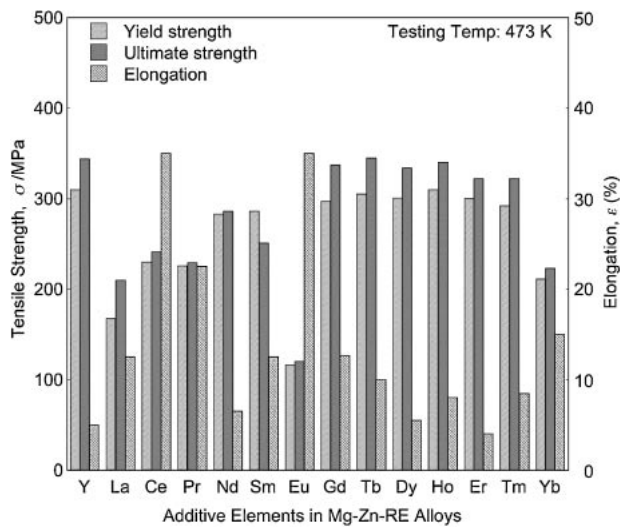


Fig. 7 Elevated-temperature tensile properties of extruded $\text{Mg}_{97}\text{Zn}_1\text{RE}_2$ alloys.

Table 1 Classification and LPSO structure of LPSO Mg-Zn-RE alloys.

	RE	as-cast	soaked
Type I	Y	18R	14H
	Dy	18R	14H
	Ho	18R + 14H	14H
	Er	18R	14H
	Tm	18R	18R
Type II	Gd	—	14H
	Tb	—	14H

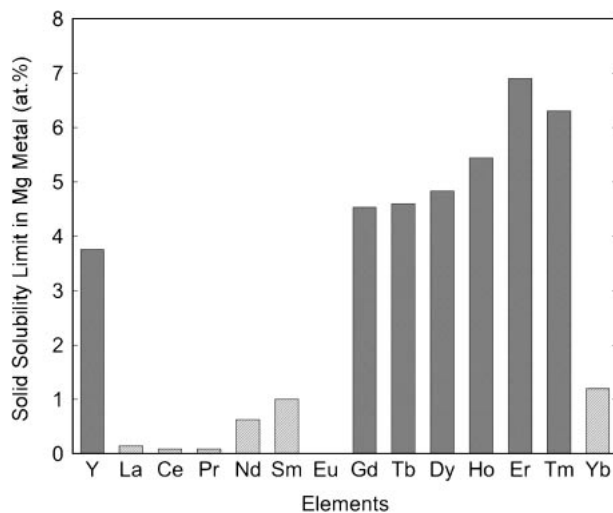


Fig. 8 The solid solubility limit of RE elements in magnesium.

(3) large solid solubility limits above approximately 3.75 at% in magnesium, and (4) larger atomic size than Mg by 8.4 to 11.9%.

4.3 Comparison of mechanical properties with conventional alloys

The tensile yield strength of the hot-extruded $\text{Mg}_{97}\text{Zn}_1\text{RE}_2$ alloys was 342 to 377 MPa, which is much higher than that of conventional high-strength magnesium alloys, such as

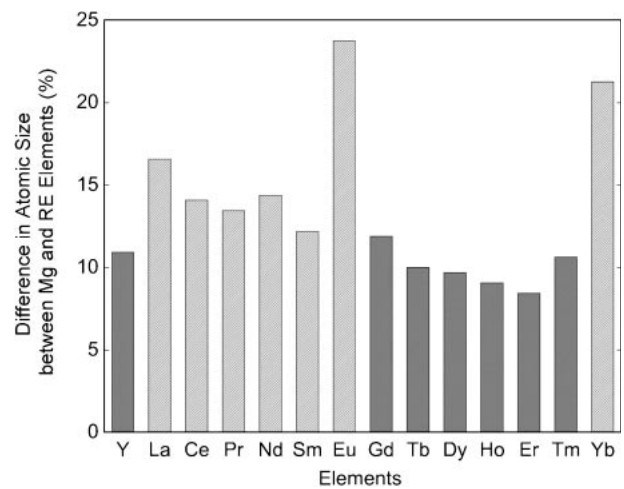


Fig. 9 The difference in atomic size between Mg and RE elements.

ZK60A-T5 extruded alloy with 285 MPa at RT, and AZ80A-T5 extruded material with 275 MPa at RT.¹⁰⁾ The elevated-temperature tensile yield strength of the wrought LPSO $\text{Mg}_{97}\text{Zn}_1\text{RE}_2$ alloys was 292 to 310 MPa at 473 K, far superior to such conventional heat-resistant magnesium alloys as WE54-T6 (180 MPa at 473 K) and QE22A-T6 (165 MPa at 473 K) containing RE elements.^{4,10)}

It has been reported that the mechanical properties of the LPSO $\text{Mg}_{97}\text{Zn}_1\text{Y}_2$ alloy were much improved by powder metallurgy processing such as the consolidation of rapidly solidified powders or chips prepared from cast ingots. The rapidly solidified powder metallurgy $\text{Mg}_{97}\text{Zn}_1\text{Y}_2$ alloy exhibits a yield strength of 610 MPa and an elongation of 5%, and the chip consolidated $\text{Mg}_{97}\text{Zn}_1\text{Y}_2$ alloy has a yield strength of 430 MPa and an elongation of 3%.^{1,6)} The effect of rapid solidification and chipping can be estimated to be increases of approximately 50% and 20% in yield strength, respectively. This improvement is due to the refinement of grain size. These powder metallurgy processes are, therefore, expected to improve the mechanical properties of the LPSO $\text{Mg}_{97}\text{Zn}_1\text{RE}_2$ alloys. Moreover, alteration of their composition has been reported to improve the mechanical properties of the LPSO Mg-Zn-Y alloys. For example, a wrought $\text{Mg}_{93.5}\text{Y}_{3.5}\text{Zn}_3$ alloy produced by hot extrusion of a cast ingot exhibits excellent tensile yield strength of 440 MPa and good ductility with 6% elongation at ambient temperature. It is, therefore, expected that LPSO Mg-Zn-RE alloys with further improved mechanical properties can be developed by optimization of alloy composition. The LPSO Mg-Zn-RE alloys are expected to find applications as practical lightweight structural materials.

5. Conclusions

We have investigated the formation and mechanical properties of $\text{Mg}_{97}\text{Zn}_1\text{RE}_2$ alloys with long-period stacking ordered (LPSO) structures by examining RE = Y, La, Ce, Pr, Sm, Nd, Gd, Dy, Ho, Er, Tb, Tm and Yb. The results are summarized as follows:

- (1) An LPSO phase was formed in $\text{Mg}_{97}\text{Zn}_1\text{RE}_2$ alloys with RE = Y, Gd, Dy, Ho, Er, Tb and Tm. Mg-Zn-Y,

Mg-Zn-Dy, Mg-Zn-Er, Mg-Zn-Ho and Mg-Zn-Tm alloys were classified as type I, in which the LPSO phase is formed during solidification. Mg-Zn-Gd and Mg-Zn-Tb alloys belong to type II, in which the LPSO phase precipitates with soaking.

- (2) The mechanical properties of hot-extruded $\text{Mg}_{97}\text{Zn}_1\text{RE}_2$ alloys with an LPSO phase included high strength and good ductility both at ambient and elevated temperatures. The yield strength, ultimate tensile strength and elongation were more than 342 MPa, 372 MPa and 3%, respectively at ambient temperature, and above 292 MPa, 322 MPa and 4%, respectively at 473 K.
- (3) The criteria for RE elements that form an LPSO phase in Mg-Zn-RE were discovered. The RE element must have a negative mixing enthalpy for the pairs Mg-RE and Zn-RE, an HCP structure at room temperature, large solid solubility limits above 3.75 at% in binary Mg-RE alloys, and an atomic size larger than Mg by 8.4 to 11.9%.
- (4) The LPSO Mg-Zn-RE alloys had excellent mechanical properties, indicating promise as lightweight structural materials.

Acknowledgements

This study was partially supported by a Grant-in-Aid for Scientific Research (A) from the Ministry of Education, Culture, Sports, Science and Technology of Japan. We wish

to thank Dr. S. Yoshimoto and Mr. Y. Nakayama for their assistance in preparing the samples.

REFERENCES

- 1) Y. Kawamura, K. Hayashi and A. Inoue: *Mater. Trans.* **42** (2001) 1171–1174.
- 2) E. Abe, Y. Kawamura, K. Hayashi and A. Inoue: *Acta Mater.* **50** (2002) 3845–3857.
- 3) D. H. Ping, K. Hono, Y. Kawamura and A. Inoue: *Philos. Mag. Lett.* **82** (2002) 543–551.
- 4) Y. Kawamura, S. Yoshimoto and M. Yamasaki: *Proc. PM2004* (European Powder Metallurgy Association, Shrewsbury, England, 2004) pp. 449–454.
- 5) T. Itoi, T. Seimiya, Y. Kawamura and M. Hirohashi: *Scr. Mater.* **51** (2004) 107–111.
- 6) Y. Kawamura and S. Yoshimoto: *Magnesium Technology 2005* (The Minerals, Metals & Materials Society, Warrendale, PA, 2005) pp. 499–502.
- 7) S. Yoshimoto, M. Yamasaki and Y. Kawamura: *Mater. Trans.* **47** (2006) 959–965.
- 8) M. Yamasaki, T. Anan, S. Yoshimoto and Y. Kawamura: *Scr. Mater.* **53** (2005) 799–803.
- 9) M. Yamasaki, M. Sasaki, M. Nishijima, K. Hiraga and Y. Kawamura: *Acta Mater.* (2007), doi: 10.1016/j.actamat.2007.08.033
- 10) *Magnesium & Magnesium alloys*, ed. by M. M. Avedesian & H. Baker, (ASM International, Materials Park, OH, 1999) pp. 3–6.
- 11) *Cohesion in Metals Transition Tetral Alloys*, ed. by F. R. de Bore *et al.*, (Elsevier Science Publishers B. V., North-Holland, 1988).
- 12) C. S. Barrett and T. B. Massalski: *Structure of Metals*, 3rd ed. (McGraw-Hill, New York, 1966).
- 13) *Phase Diagrams of Binary Magnesium Alloys*, eds. A. A. Nayeb-Hashemi and J. B. Clark, (ASM International, Metals Park, Ohio, 1988).